31st Annual International Conference of the IEEE EMBS
Minneapolis, Minnesota, USA, September 2-6, 2009

Multi-Image Registration for Evaluating the 99mTc-TRODAT-1 of Parkinson's Rat Model

Jiann-Der Lee, Yi-Hsuan Chu, Cheng-Wei Chen and Kun-Ju Lin

Department of Electrical Engineering, Chang Gung University, Taiwan 333

***Abstract*—Study on small animal model using multiple imaging is an important procedure in medicine and physiology. Recently, Single Photon Emission Computed Tomography (SPECT) of dopamine transporter with ^{99cm}Tc-TRODA-1 has been proved to be a valuable and feasible mean of assessing the integrity of dopamine neurons. In this paper, an image registration algorithm for MRI and SPECT is proposed to evaluate the changes of a Parkinson's rat in brain organization and function. In addition, an automatic labeling algorithm which highlights striatum is necessary because manually segmenting these tissues from MRI is usually time consuming. As a result, we have built a computer-aid clinical diagnosis system which automates all the processes. This paper provides effective evaluation of Parkinson's symptoms by calculating the values of binding potentials for dopamine for quantification. Experimental result shows that the performance of the proposed method is better than the previous approach based on automated image registration.**

I. INTRODUCTION

With the aid of CT, MRI and SPECT imaging, the structure and function of the brain has become ever more transparent and the information derived from these images are useful in the clinical diagnosis of neurological disease. Generally, the CT image is primarily useful for visualizing the structure of the brain. SPECT can reveal the functional neurobiological metabolic changes and neurochemistry. MRI makes it possible to obtain structural tissue from any slices, as well as many other physical reference data. So the multimodal comparison of the CT, SPECT, and MRI is helpful to realize a complete picture of the soft tissue regions.

Parkinson's disease (PD) is a progressively neuro-degenerative disorder characterized by symptoms, including akinesia, rigidity and tremors. In the clinical application of PD, functional imaging techniques such as single photon emission computed tomography (SPECT) provides useful information for detecting in vivo metabolic and neuro-chemical changes characterizing of PD pathology.

This work was partially supported by National Science Council, R.O.C. under Grant 95-2221–E182-033-MY3 and Molecular Imaging Center, Chang Gung Memorial Hospital

Jiann-Der Lee is with the Department of Electrical Engineering, Chang-Gung University, Tao-Yuan, Taiwan 333, R.O.C. (corresponding author to provide e-mail: jdlee@mail.cgu.edu.tw).

Cheng-Wei Chen and Yi-Hsuan Chu are with Chang-Gung University, Tao-Yuan, Taiwan 333, R.O.C.

Recent researches have shown that ^{99cm}Tc-TRODAT-1 is useful in the diagnosis of PD [1] because TRODAT-1 can bind to the dopamine transporter sites at pre-synaptic neuron membrane and can easily be labeled with ^{99cm}Tc. For example, observe the T2-Weighted MRI as shown in Fig.1(a) it is difficult to differentiate the healthy mouse brain from that of the mouse with Parkinson's, but with use of the ^{99cm}Tc contrast medium the SPECT can very clearly distinguish the pathological Parkinson's mouse from the healthy mouse, as seen in Fig.1(b) and Fig.1(c), respectively. Thus the ^{99cm}Tc -TRODA-1 has been clinically proven to improve diagnosis of the condition of dopamine neuron.

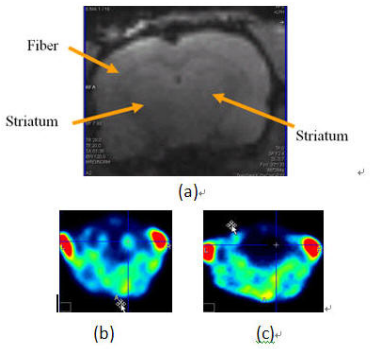

Fig.1 Example of T_2-Weighted MRI and ^{99m}Tc-TRODA-1 SPECT (a) MRI Image (b) SPECT image from a healthy mouse (c) SPECT image from a Parkinson's mouse.

According to previous literature, it is found that the prior art for small animal medical imagery primarily consisted of automated image registration (AIR) [2]-[3] and the mutual information (MI) [4]-[6]. Nevertheless, these methods were unstable when nonbrain structures were not removed before performing registration process. To alleviate this, we propose a deformable registration algorithm for MRI labeling before MRI/SPECT registration.

Here, we formulated the MRI labeling problem as a deformable-registration-based segmentation. First, manual labeling of the ROIs is really a heavy and complicated task especially for tons of patient's images. Second, only one SPECT slice with the highest activity is concerned in computing binding index because it is difficult to accomplish the labeling of the whole MRI image set. Third, an accurate and reliable MRI/SPECT registration is also necessary. Then a computer-aided system, which comprises MRI labeling of

ROIs and MRI/SPECT registration, has been developed for the evaluation of Parkinson's disease.

First of the proposed registration scheme, one set of MRI with pre-selected ROI in the striatum were used as templates. MRI image of other mice are find striatum utilizing the template. Next, the SPECT and MRI are combined to determine the precise SPECT distribution and location of the striatum, and then the Binding Ratio (BR) as clinical standards were employed to evaluate the changes of a Parkinson's rat in brain organization and function. Here, let R_{CP} stands for striatum and R_{OCC} stands for the occipital cortex as the background. The binding ratio (BR) is calculated by the Eq. 1

$$BR= (R_{CP}-R_{OCC})/ R_{OCC} \quad (1)$$

Where R_{CP} and R_{OCC} represents the mean counts per voxel within the *cp* and *occ*, respectively.

II. The Proposed System

The proposed system comprises three components: (1) MRI Image labeling (2) MRI/SPECT registration (3) Clinical evaluation of Parkinson's. The flowchart of the proposed system is given in Fig. 2. Two 3-D image sets, MRI and SPECT which were scanned from the same mouse, are imported. MRI is then labeled by elastically registering with a labeled MRI template. Afterward, performing a rigid registration of MRI and SPECT results a transformation for transforming SPECT onto the MRI. Therefore, MRI and SPECT are registered and the binding ration of ROIs can be obtained by calculating the intensity of SPECT within the labeled regions of MRI. The two key modules, MRI/SPECT registration and MRI labeling, are detailed in the following sections.

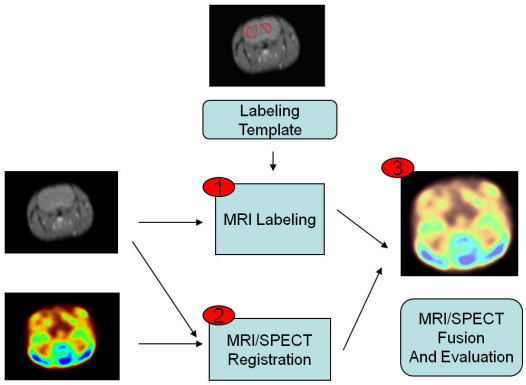

Fig. 2 The flowchart of the proposed system

A. Clinical MRI and SPECT data

In this study, all experiments were carried out in a similar manner using a mouse head (mouse, 20–30 g, three healthy mice and three mice with Parkinson's) as the imaging target. In each study, the mouse was injected with the radionuclide ^{99m}Tc-TTRODA, at a dosage of 2.95 mci, with a half-life for the ^{99m}Tc-TRODA of 90min. The Nano SPECT/CT and 3T-MRI were used to obtain SPECT and MRI images of the mice, respectively. The resolution of SPECT image is 170*170*152 voxels, and the MRI image is 384*128*16 voxels. The reconstructed data of SPECT was provided by Chang Gung Memorial Hospital, Lin-Kou, Taiwan, using their standard injection and reconstruction protocol.

B. MRI/SPECT registration

In order to calculate the specific-to-nonspecific binding ratio of the nuclear medical, registering MRI and SPECT image is a significant process. Therefore, an automated MRI/SPECT image registration algorithm of using an adaptive similarity metric proposed in our previous work [7] is used here. The proposed registration framework is based on the framework proposed by Maes [8], the principal aspect of which is reliance on the image intensity as the foundation, and then applying optimization algorithms to ascertain commonalities by the spatial similarity method to optimize the result. For this, we employ Studholme's [9] (Normalized Mutual Information (NMI) to serve as the similarity metric method, as this method has the advantage of avoiding overlap. Optimization algorithms search for optimal solutions in the solution set, Powell's algorithm is one of the methods used in solving optimization problems, the main technique of which is to first select a search direction, then begin from a starting point using the search for an objective function for minimization in this direction, and then using that point as a new starting point, repeating the process until arriving at an adequate solution, the advantage being that one need not calculate a differential equation for the objective function, but rather can find a result by limited repetitive steps. For this, we assume the objective function F is a function with n dimensions χ_k, k =1,…, n , to find the optimum for χ_k, Powell's algorithm uses the following steps to find the optimal solution:

1. Let k = 1.
2. Assume other parameters are fixed, except χ_k.
3. Find χ_k' in solution space of χ_k. to optimize the function *F*.
4. Let $\chi_k = \chi_k$',and $k= k+1$.
5. Repeat steps 2-5 until the stop criterion is met.

C. Image Labeling

We formulate the MRI labeling as an deformable-registration-based segmentation problem. The flowchart of this deformable registration is illustrated in Fig. 3. Denote $f_A(i)$ and $f_B(i)$ as the reference image A and the floating image B, respectively, where $i \in I \subset R^N$. I is an N-dimensional discrete interval representing the set of all pixel coordinates in the image. Suppose the deformable image is a geometrically deformed version of the reference image, and vice versa. Therefore, registering A and B is equivalent to estimating a deformation function $\hat{u}$ by optimizing a similarity metric, SM, as the Eq. 2:

$$\hat{u} = \arg\underset{u}{opt}\, SM(f_A(t), f_B^w(t)) \quad (2)$$

$$f_B^w(t) = f_B(u(t)) \quad (3)$$

where t represents the point with the same coordinate in the reference image and in the warped deformed image $f_B^w(t)$. The Normalized Mutual Information [9] is used as the similarity metric and the Free-Form Deformation (FFD) [10] is utilized to model the deformable field in this research.

It is noted that a coarse-to-fine strategy is used to reduce computing cost during the optimization process. By finding a number of corresponding control points in the images first and then use information about the correspondences to interpolate a transformation function which determines the spatial correspondence between all points in the images. Finally, the warped moving image can be interpolated by a cubic B-spline [11] defined by Eq. 4. As a result, a smoothness constrain is then involved in the framework of deformable registration, resulting in a smooth and continuous deformation. Eq. 5 shows a smoothness cost function which sums the differentials of u by x, y and z, respectively. In summary, the registration problem is an optimization problem that optimizes a cost function C consisting a similarity metric term $C_{similarity}$ and a smoothness term $C_{curvature}$, as shown in Eq. 6

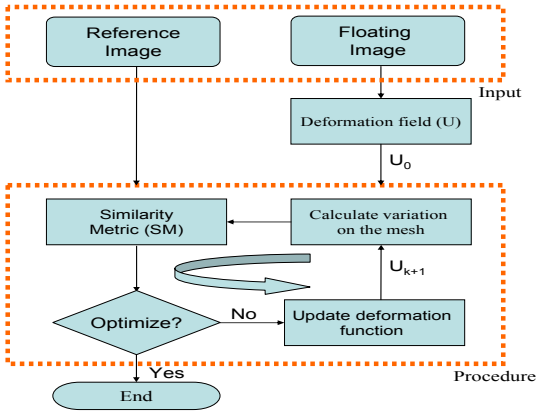

Fig. 3 The flowchart of the deformable registration algorithm

$$u(x,y) = \sum_{m=0}^{3}\sum_{n=0}^{3} \theta_m(p)\theta_n(q)\phi_{i+m,j+n} \quad (4)$$

where $i = \left\lfloor \frac{x}{\delta} \right\rfloor - 1$, $j = \left\lfloor \frac{y}{\delta} \right\rfloor - 1$, $p = \frac{x}{\delta} - \left\lfloor \frac{x}{\delta} \right\rfloor$, $q = \frac{y}{\delta} - \left\lfloor \frac{y}{\delta} \right\rfloor$ and θ_m represents the m-th basis function of the cubic B-splines:

$$\theta_0(s) = (1-s)^3/6$$

$$\theta_1(s) = (3s^3 - 6s^2 + 4)/6$$

$$\theta_2(s) = (-3s^3 + 3s^2 + 3s + 1)/6$$

$$\theta_3(s) = s^3/6$$

$$C_{curvature} = \int_{-\infty}^{\infty}\int_{-\infty}^{\infty}\int_{-\infty}^{\infty} [(\frac{\partial U}{\partial x})^2 + (\frac{\partial U}{\partial y})^2 + (\frac{\partial U}{\partial z})^2]dx\ dy\ dz \quad (5)$$

$$U_{k+1} = \arg\max_{U}(\omega_1 \times C_{similarity}(U) - \omega_2 \times C_{curvature}(U)) \quad (6)$$

III. Experimental Results

A. The validity of MRI labeling

In order to validate the automatic MRI labeling procedure by using a deformable registration algorithm, we compared the results with those of manually labeling the datasets. The results of the manual segmentation were accomplished by an experienced user and are regarded as a ground truth. Each of the labeled results was then compared to every other using two criteria for quantifying reliability, percent volume overlap (PVO) and percent volume difference (PVD) [12] as shown in Eq. (7) and Eq. (8), among these suppose that there are two already labeled structures S_1 and S_2 respectively. In other words, S_1 stands for the segmented result from an experienced user, and S_2 stands for the segmented result using the proposed optimization algorithm. $V(S)$ is the volume of S, $O(S_1, S_2)$ denotes the PVO between the two regions, and $D(S_1, S_2)$ denotes the PVD between the two regions. The labeling results of normal mice and PD mice are listed in Table 1and Table 2, respectively

$$O(S_1, S_2) = \frac{V(S_1 \cap S_2)}{(V(S_1) + V(S_2)/2)} \times 100\% \quad (7)$$

$$D(S_1, S_2) = \frac{|V(S_1) - V(S_2)|}{(V(S_1) + V(S_2)/2)} \times 100\% \quad (8)$$

Table 1: The labeling result of normal mice

	PVO(%)	PVD(%)
Left Striatum	94.43	3.24
Right Striatum	89.66	3.52

Table 2: The labeling result of PD mice

	PVO(%)	PVD(%)
Left Striatum	79.01	11.85
Right Striatum	83.81	12.32

Using the proposed registration method, the result is shown in Fig. 4

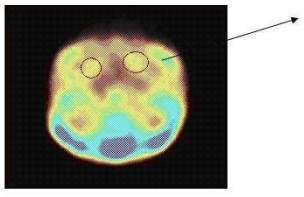

Fig. 4 MRI/SPECT Registration Result

B. Clinical Evaluation

Since MPTP (1-methy1-4pheny1-1, 2, 3, 6-tetrahydropyridine, MPTP) neurotoxin will destroy the dopamine neuron of the brain, we inject it to the mice to

produce Parkinson's symptoms. The experiment involves the following steps for two groups, one are the normal mice. For which we inject twice daily with PBS(Phosphate Buffer Solution) each injection is four hours apart for five days total. The other groups are the Parkinson's rats, which are injected with a combination of MPTP and PBS, and this will induce Parkinson-like symptoms. Table 3 and Table 4 show the Binding Ratio (BR) for the healthy and Parkinson's mice, respectively. The results show the normal rats are about 2.3 while the Parkinson's rats depend on the length of time since injection, but clearly the results show after five days' injection the dopamine has been reduced. With greater deduction in dopamine over time and mice movement was also slower over time. And there were clinical signs of tremors.

Table 3: The mean error of Binding Ratio of Normal mice control group at specific regions (inject with PBS for five days)

pixels	Inject for the third day	Second day when finished	Ninth day when finished
R_{cp}	40	37	39
R_{occ}	12	11	12
BR	2.33	2.36	2.25

Table 4: The mean error of Binding Ratio of PD mice control group at specific regions (inject a combination of MPTP and PBS for five days)

pixels	Inject for the third day	Second day when finished	Ninth day when finished
R_{cp}	24	19	17
R_{occ}	11	11	11
BR	1.18	0.73	0.54

IV. Conclusion

In this paper, we have proposed an image registration algorithm for MRI/SPECT and image labeling, which provides effective evaluation of Parkinson's symptoms by calculating the values of binding potentials for dopamine for quantification. We have built a computer-aided diagnosis system which automates the whole process of evaluating 99mTc-TRODAT-1 SPECT. Two main functions are integrated into this system: one is an automatic ROI labeling by using a deformable registration, and the other is an automatic MRI/SPECT registration.

Acknowledgments. We are thankful to Prof. Jin-Chung Chen for experiment set up and technical assistance. This work was supported by Ministry of Economic Affairs, Taiwan under Technology Development Program for Academia (TDPA) with Grant No. 95-EC-17-A-19-S1-035.

References

[1] Y. H. Weng, T. C. Yen, M. C. Chen, P. F. Kao, K. Y. Tzen, R. S. Chen, "Sensitivity and specificity of 99mTc-TRODAT-1 SPECT imaging in differentiating patients with idiopathic Parkinson's disease from healthy subjects," J. Nucl Med, vol. 45, pp. 393-401, 2004

[2] R. P. Woods, J. C. Mazziotta, and S. R. Cherry, "MRI-PET Registration with Automated Algorithm," Journal of Computer Assisted Tomography, vol.17, pp. 536-546 , 1993

[3] J. J Vaquero, M. Desco, J Pascau, A. Santos, I. J, Lee, J. Seidel and M. V. Green, "PET and CT image registration of the rat brain and skull using the AIR algorithm," Nuclear Science Symposium Conference Record, vol.3, pp. 16/22-16/23 , 2000

[4] W. M. Wells, P. Viola, H. Atsumi, S. Nakajima, and S. Kikinis, "Multi-modality volume registration by maximization of mutual Information," IEEE Trans. on medical imaging, vol.1, pp. 35-51 , 1996

[5] J. J. Vaquero, et al., "PET, CT, and MR image registration of the rat brain and skull," IEEE Trans. on Nuclear Science, vol.48, pp. 1440-1445 , 2001

[6] G. J. Topping et al, "Methods for Parkinson's rat model PET image analysis with Region of Interest," Proceeding of 2007 IEEE Nuclear Science Symposium, vol.4, pp. 2917-2921 , 2007

[7] J. D. Lee, C. H, Huang, C. W. Chen, Y. H. Weng, K. J. Lin, and C. T. Chen, "Brain MRI/SPECT Registration System Using an Adaptive Similarity Metric : Application on the Evaluation of Parkinson's Disease," Proceeding of MIRAGE 2007, LNCS 4418, pp. 235-246, 2007.

[8] F. Maes, A. Collignon, D. Vandermeulen, G. Marchal and P. Suetens, "Multimodality image registration by maximization of mutual information," IEEE Transaction on Medical Imaging, vol.16, pp. 187-198 , 1997

[9] C. Studholme, D. L. G. Hill and D. J. Hawkes, "An overlap invariant entropy measure of 3D medical alignment," Pattern Recognition, vol. 32, pp. 71-86 , 1999

[10] T.W. Sederberg and S.R. Parry. "Free-form deformation of solid geometric models," In Proceedings of SIGGRAPH'86, Computer Graphics, pages 151-160, 1992

[11] J. V. Hajna, D. L. G. Hill, and D. J. Hawkes, Eds. "Medical Image Registration," Boca Roton FL: CRC, 2001.

[12] D.L. Collins, W. Dai, T. Peter, and A. Evans, "Automatic 3D Model-based neuroanatomical segmentation," Hum Brain Mapp, vol. 3, pp. 190-208, 1995